Received: 20 February 2018 | Revised: 4 April 2018 | Accepted: 5 April 2018

DOI: 10.1111/gcb.14273

PRIMARY RESEARCH ARTICLE

WILEY Global Change Biology

Disentangling the effects of acidic air pollution, atmospheric CO_2, and climate change on recent growth of red spruce trees in the Central Appalachian Mountains

Justin M. Mathias | Richard B. Thomas

Department of Biology, West Virginia University, Morgantown, West Virginia

Correspondence
Justin M. Mathias, Department of Biology, West Virginia University, Morgantown, WV.
Email: jmathia6@mix.wvu.edu

Funding information
National Science Foundation, Grant/Award Number: 1354689

Abstract

In the 45 years after legislation of the Clean Air Act, there has been tremendous progress in reducing acidic air pollutants in the eastern United States, yet limited evidence exists that cleaner air has improved forest health. Here, we investigate the influence of recent environmental changes on the growth and physiology of red spruce (*Picea rubens* Sarg.) trees, a key indicator species of forest health, spanning three locations along a 100 km transect in the Central Appalachian Mountains. We incorporated a multiproxy approach using 75-year tree ring chronologies of basal tree growth, carbon isotope discrimination ($\Delta^{13}C$, a proxy for leaf gas exchange), and $\delta^{15}N$ (a proxy for ecosystem N status) to examine tree and ecosystem level responses to environmental change. Results reveal the two most important factors driving increased tree growth since *ca.* 1989 are reductions in acidic sulfur pollution and increases in atmospheric CO_2, while reductions in pollutant emissions of NO_x and warmer springs played smaller, but significant roles. Tree ring $\Delta^{13}C$ signatures increased significantly since 1989, concurrently with significant declines in tree ring $\delta^{15}N$ signatures. These isotope chronologies provide strong evidence that simultaneous changes in C and N cycling, including greater photosynthesis and stomatal conductance of trees and increases in ecosystem N retention, were related to recent increases in red spruce tree growth and are consequential to ecosystem recovery from acidic pollution. Intrinsic water use efficiency (*i*WUE) of the red spruce trees increased by ~51% across the 75-year chronology, and was driven by changes in atmospheric CO_2 and acid pollution, but *i*WUE was not linked to recent increases in tree growth. This study documents the complex environmental interactions that have contributed to the recovery of red spruce forest ecosystems from pervasive acidic air pollution beginning in 1989, about 15 years after acidic pollutants started to decline in the United States.

KEYWORDS
acid deposition, carbon isotopes, elevated CO_2, intrinsic water use efficiency, nitrogen isotopes, *Picea rubens*, tree growth, tree rings

1 | INTRODUCTION

Recent observations of enhanced tree growth in temperate forest ecosystems of the northern hemisphere have raised questions about the underlying causal mechanisms (Boisvenue & Running, 2006; Engel et al., 2016; Fang et al., 2014; Johnson & Abrams, 2009; McMahon, Parker, & Miller, 2010; Thomas, Spal, Smith, & Nippert, 2013). Is this increased productivity a consequence of forest regrowth following disturbance, or is tree growth being enhanced by environmental changes, such as CO_2 fertilization and climate change (Joos, Prentice, & House, 2002; Schimel et al., 2000)? These are critical questions because forest ecosystems are a significant part of the terrestrial carbon (C) sink that removes nearly 30% of anthropogenic C emissions each year, providing a negative feedback that moderates climate change (Le Quéré et al., 2018). Yet, a large amount of uncertainty exists about the continued capacity of forests to sequester C emissions (Friedlingstein et al., 2006). Initially, forest regrowth after disturbance provides a large C sink, but this sink may not persist as forest productivity slows during the late stages of stand development, thereby limiting the capacity of the C sink (Caspersen et al., 2000; Fang et al., 2014). The persistence of the effects of increased CO_2 and climate change on forest C sequestration are harder to predict and are likely to interact with the dynamics of forest recovery, possibly resulting in either positive or negative feedbacks on the C sink (Anderson-Teixeira et al., 2013). In order to partition the relative contributions by these drivers, and how their complex interactions affect forest C sinks, we need a deeper understanding of how simultaneous changes in key environmental variables affect long-term C cycling in forest ecosystems.

For decades, temperate forests in the eastern United States have experienced anthropogenic disturbance, including pervasive levels of acidic air pollution from fossil fuel combustion (Greaver et al., 2012). Before environmental legislation designed to curb pollutant emissions became effective, national levels of SO_2 and NO_x emissions were as high as 29.6 and 25.6 million metric tons annually (Lefohn, Husar, & Husar, 1999; EPA, 2015) (Figure S1a,b). Since the Clean Air Act and subsequent amendments, SO_2 and NO_x emissions have fallen from their highest levels by 84% and 56%, respectively (Lefohn et al., 1999; EPA, 2015). Although significant progress has been made in understanding C cycling following many types of disturbance in forest ecosystems (Liu et al., 2011), mechanisms that govern recovery from acid deposition following reductions in acidic air pollution are still poorly understood. It has been projected that the recovery of terrestrial ecosystems following long-term acid deposition takes decades (Driscoll et al., 2001; Likens, Driscoll, & Buso, 1996), and now over four decades after the Clean Air Act of 1970, there remains scant evidence of forest ecosystem recovery from the long history of disturbance by acid deposition in the eastern United States. (Engel et al., 2016; Lawrence et al., 2015; Li et al., 2010; Thomas et al., 2013).

In addition to the declines in acidic air pollution since the Clean Air Act, there have been substantial increases in atmospheric CO_2 concentrations (Figure S1c), along with significant changes in climate (Figure S1d). Increasing atmospheric CO_2 concentrations stimulates forest productivity, thereby enhancing carbon storage (Fernández-Martínez et al., 2017; Norby et al., 2005); however, these responses are often modulated by changes in temperature or precipitation (Granda, Rossatto, Camarero, Voltas, & Valladares, 2014; Jennings, Guerrieri, Vadeboncoeur, & Asbjornsen, 2016), in addition to acid pollutants (Fernández-Martínez et al., 2017). It is, therefore, critical to understand how each of these factors contribute to the recovery of trees from acid pollution and the extent, and nature, of any interactive effects between tree recovery and environmental change.

Tree ring growth and isotope chronologies have become important proxies used to examine historical changes in productivity, plant physiology, and ecosystem processes in a rapidly changing environment (Dye et al., 2016; McLauchlan et al., 2017; Thomas et al., 2013). While tree ring chronologies provide an opportunity to examine changes in forest productivity (Dye et al., 2016), these datasets are strengthened by linking observed changes in growth to underlying physiology (Belmecheri et al., 2014; Thomas et al., 2013). In particular, carbon isotope signatures of tree rings provide information regarding the diffusive and biochemical processes of photosynthesis (Farquhar, Ehleringer, & Hubick, 1989; Farquhar, O'Leary, & Berry, 1982). Nitrogen isotope signatures ($\delta^{15}N$) of tree rings record changes in ecosystem N status, although the exact mechanisms have yet to be fully reconciled (Evans, 2001; Gerhart & McLauchlan, 2014). It has been postulated that tree ring $\delta^{15}N$ reflects pollutant emissions and deposition of oxidized N compounds (Elliott et al., 2007; Gurmesa et al., 2017; Hietz, Dünisch, & Wanek, 2010); however, there is also abundant evidence that $\delta^{15}N$ reflects ecosystem N cycling dynamics (Burnham, McNeil, Adams, & Peterjohn, 2016; Craine et al., 2009, 2015; Evans, 2001, 2007; Hobbie & Högberg, 2012; McLauchlan et al., 2017; Nadelhoffer & Fry, 1994). These proxies become more informative when an integrative approach is taken, combining multiple indicators of ecosystem status in order to track long-term changes in ecosystem function (Choi, Lee, Chang, & Ro, 2005; Kwak, Lim, Chang, Lee, & Choi, 2011; Leonelli et al., 2012; Zeng, Liu, Xu, Wang, & An, 2014).

For this study, we incorporated a multiproxy approach, using tree ring basal area increment (BAI), $\Delta^{13}C$, and $\delta^{15}N$ to explore the drivers of recent growth and physiological changes of red spruce trees (*Picea rubens* Sarg.), an economically and ecologically important conifer species in temperate forests of the eastern United States and a key indicator species of forest disturbance by acidic air pollution (Hamburg & Cogbill, 1988; Johnson & Siccama, 1983; Siccama, Bliss, & Vogelmann, 1982). Our objectives were to (1) identify those factors most related to proximate increases in red spruce growth in the Central Appalachian Mountains; (2) examine the relationships between tree growth, reconstructed seasonally integrated leaf physiology, including *i*WUE, and environmental factors; and (3) explore the use of tree ring $\delta^{15}N$ as an integrator of historical ecosystem N cycling. To meet these objectives, we examined red spruce tree growth using tree rings at three forest locations spanning a 100 km transect in the Central Appalachian Mountains where we have previously examined drivers of ecosystem N availability (Smith, Mathias, McNeil, Peterjohn, &

Thomas, 2016). We used Kendall's rank correlation analyses and generalized linear mixed models (GLMMs) to disentangle the multiple environmental effects and their sensitivities on red spruce tree growth into discreet components.

2 | MATERIALS AND METHODS

2.1 | Study locations and red spruce tree growth analyses

Three red spruce forest stands were chosen along a north–south transect of 100 km along the Central Appalachian Mountains. McGowan Mountain (MCG; 38°58′N, 79°41′W) is positioned within the Appalachian Plateau physiographic province, while Span Oak Run (SOR; 38°37′N, 79°46′W), and Cranberry Glades (CGL; 38°12′N, 80°17′W) are located in the Allegheny Mountain Section physiographic province of West Virginia (USGS, 1946). Each site is ≥900 meters in elevation and has a southwest aspect with slopes ranging from 0% to 10%. The mean annual temperature for this region in West Virginia was 9.5°C over the period of 1940–2014 (WV Climate Division 4, NOAA, 2017). The annual total precipitation across this time period was 1229.6 mm/year, with 47% of the precipitation during the growing season from May to September (WV Climate Division 4, NOAA, 2017). Soils at each of the three sites consist of a thick organic layer with litter contributed by red spruce (*Picea rubens* Sarg.), eastern hemlock (*Tsuga candadensis*), yellow birch (*Betula alleghaniensis*), and red maple (*Acer rubrum*) as dominant canopy species. These sites are mature closed canopy stands with no evidence of anthropogenic or natural disturbance, such as logging or fire, since logging events in the early 1900s. Overall tree density at MCG, SOR, and CGL was 534, 617, and 675 trees/ha, with red spruce contributing *ca.* 23%, 25%, and 48% of the trees, respectively. Soils at MCG are classified as ernest and are moderately well to poorly drained, very deep, and have parent material that is colluvium derived from acid shale, siltstone, and sandstone (USDA Soil Survey Geographic (SSURGO), 2015). SOR and CGL are snowdog series soils and are very deep, moderately well drained, and colluvium derived from acid sandstone, siltstone, and shale (USDA Soil Survey Geographic (SSURGO), 2015). The underlying geology at MCG and CGL consists of Pennsylvanian Pottsville sandstone, while SOR is underlain by Devonian Chemung Shale (WVGES, 1968). Thus, the soil buffering capacities are different at each site with MCG having the lowest buffering capacity and CGL having the greatest buffering capacity.

At each site, 20–25 red spruce trees, greater than 10 cm diameter at breast height (1.4 m aboveground), were cored using a 5.15 mm increment borer (Haglöf Inc., Madison, MS). Trees were randomly selected to avoid any potential biases during growth analyses, and cores were taken perpendicular to the slope to avoid compression and expansion wood. Twenty cores from MCG were harvested at the end of the 2013 growing season, with five additional cores harvested after the 2014 growing season. At SOR and CGL, all tree cores were collected at the end of the 2014 growing season. Cores were returned to lab where they were processed according to standard dendrochronological techniques, as described by Stokes and Smiley (Stokes & Smiley, 1996). Chronologies were crossdated using WinDENDRO (Regent Instruments, Inc.), and statistically confirmed using dplR (Bunn et al., 2015), after which an individual calendar year was assigned to each growth ring. The average age of sampled red spruce trees from the three locations was 109 ± 27 years (mean ± *SD*). The early portion of the tree ring chronologies represented growth release of saplings after logging in the early 1900s and therefore, the focus of this study was the time period after juvenile growth, 1940–2014. The expressed population signals (EPS), a measure of the common variance in a chronology, for each red spruce site across years 1940–2014 were all greater than 0.85, indicating that our sample size adequately represents the tree population (Wigley, Briffa, & Jones, 1984). Raw ring widths of each year were converted to basal area increment (BAI) to better characterize tree growth and to minimize the effects of tree size and age on annual growth trends using

$$\mathrm{BAI} = \pi(R_n^2 - R_{n-1}^2), \tag{1}$$

where R is the radius of the tree at a given year of ring formation, n. At each site, BAI was averaged for each year using the 20–25 red spruce trees at each location to develop site-level chronologies, which we treated as replicates (N = 3) in this study.

2.2 | Isotopic analysis of tree rings

A subset of five randomly chosen tree cores was selected from each location to develop C and N isotope chronologies for the red spruce trees. As with BAI, C and N isotopes were averaged for similar years and forest site was a replicate (N = 3). Samples were analyzed for their stable C or N isotope composition with a ThermoFisher Delta V+ isotope ratio mass spectrometer interfaced with a Carlo Erba NC 2500 Elemental Analyzer. For these analyses, tree cores were dissected under microscope by scalpel into individual growth rings at the boundary of earlywood and latewood for years 1940–2014. Tree ring whole wood from each individual year was then finely chopped to homogenize the sample, and 1 ± 0.2 mg was packed into tin capsules for C isotopic analysis. Carbon isotope composition was measured as $\delta^{13}C$ (‰) using

$$\delta^{13}C‰ = (R_{\mathrm{sample}}/R_{\mathrm{standard}} - 1) * 1{,}000, \tag{2}$$

where R_{sample} is the ratio of ^{13}C:^{12}C in the wood sample and R_{standard} is the ratio of ^{13}C:^{12}C in the standard PeeDee belemnite (PDB) from the PeeDee River Formation in Hemingway, South Carolina. The conversion of leaf carbohydrate to wood was then accounted for by subtracting 3‰ from the wood $\delta^{13}C$ (Leavitt & Long, 1982; Thomas et al., 2013). Leaf-corrected $\delta^{13}C$ values were converted to isotope discrimination ($\Delta^{13}C$) to account for the progressive depletion in atmospheric $\delta^{13}CO_2$ due to fossil fuel burning using

$$\Delta^{13}C = \left(\frac{\delta^{13}C_{\mathrm{air}} - \delta^{13}C_{\mathrm{plant}}}{1 + \frac{\delta^{13}C_{\mathrm{plant}}}{1{,}000}}\right), \tag{3}$$

where $\delta^{13}C_{\mathrm{air}}$ and $\delta^{13}C_{\mathrm{plant}}$ are the stable carbon isotope compositions of the atmosphere and plant, respectively (Farquhar et al.,

1982). Atmospheric $\delta^{13}C$ values for a given year up to 2004 used to calculate $\Delta^{13}C$ were interpolated using the high precision records of atmospheric $\delta^{13}C$ obtained from Antarctic ice cores (Francey et al., 1999) by McCarroll and Loader (2004). After 2004, atmospheric $\delta^{13}C$ was calculated as the average change per year (−0.0199‰) during the 1940–2004 period (Keeling, Piper, Bollenbacher, & Walker, 2010). For this study, needle structure, mesophyll conductance, and mesophyll CO_2 fractionation of red spruce trees were assumed to have not changed across the 75-year tree ring chronology (Seibt, Rajabi, Griffiths, & Berry, 2008).

For N isotope samples, whole wood for three consecutive years was combined (e.g., 1941, 1942, and 1943 are designated as 1942) to ensure an adequate sample mass for analysis (~10 mg) given the low N concentration in wood and, therefore, represent a wood N isotope signal integrated over 3 years. Wood nitrogen isotope composition was measured as $\delta^{15}N$ (‰) using

$$\delta^{15}N(‰) = (R_{sample}/R_{standard} - 1) * 1000, \quad (4)$$

where R_{sample} is the ratio of ^{15}N:^{14}N in the wood sample and $R_{standard}$ is the ratio of ^{15}N:^{14}N in atmospheric N_2.

2.3 | Reconstruction of photosynthetic parameters across the chronology

In order to simulate changes in seasonally integrated photosynthesis (A), stomatal conductance (g_c), and intrinsic water use efficiency (iWUE) across the tree ring chronology from 1940 to 2014, field measurements of the relationship between A and leaf intercellular CO_2 (C_i) (A–C_i curves) were coupled with the $\Delta^{13}C$ chronology, following the methods of (Thomas et al., 2013). First, $\Delta^{13}C$ was converted to C_i/C_a, the ratio of leaf intercellular CO_2 to atmospheric CO_2, using

$$\frac{C_i}{C_a} = \frac{\Delta^{13}C - a}{b - a}, \quad (5)$$

where a is the diffusional fractionation of CO_2 through the stomata (4.4‰) and b is the biochemical fractionation of CO_2 by Rubisco (27‰) (Farquhar et al., 1982). For each individual year of the chronology, the respective C_i/C_a was multiplied by the atmospheric CO_2 concentration (Keeling, Piper, Bollenbacher, & Walker, 2015) to determine C_i. Values of isotopically derived C_i were then used to predict the seasonally integrated A using A-C_i relationships derived from measurements at each of our three sites. Stomatal conductance was calculated using methods from (Farquhar & Sharkey, 1982) using

$$g_c = \left|\frac{O - A}{C_a - C_i}\right|, \quad (6)$$

where A is seasonally integrated photosynthesis, C_a is the atmospheric CO_2 concentration and C_i is the leaf intercellular CO_2 concentration.

For the calculation of A and g_c, we measured A-C_i response curves from at least three red spruce trees per site during June, July, and August 2014. Between 0900 and 1600 EST, we harvested small branches containing intact sun needles from the upper canopy and immediately placed them into water picks to maintain the transpiration stream. A-C_i curves were measured using an open-flow gas exchange system with red/blue LED lights (LI6400XT, Li-Cor, Inc., Lincoln, NE) by placing intact needles into the cuvette at saturating light (1,500 μmol photons m^{-2} s^{-1}). After *ca.* 5 min equilibration in the cuvette, rates of photosynthesis were measured at nine ambient CO_2 concentrations between 50 and 1,200 μl CO_2 L^{-1} air beginning at ambient CO_2 (400 ppm) at the time of the study. After gas exchange analyses, all needles were taken to the laboratory and scanned to determine projected leaf area, and gas exchange of red spruce was expressed on a total leaf area basis.

Intrinsic water use efficiency was calculated using C_i and C_a where

$$iWUE = \frac{A}{g_s} = (C_a - C_i) * 0.625, \quad (7)$$

whereby Fick's law of diffusion of CO_2 into the leaf is solved for the quantity $\frac{A}{g_c}$ and g_c is converted to stomatal conductance to water (g_s) by accounting for the different diffusivities of H_2O and CO_2 (Farquhar et al., 1989).

2.4 | Statistical analyses

Breakpoint analyses were performed using the R package 'segmented' (Muggeo, 2008) with the red spruce chronologies of BAI, $\Delta^{13}C$, and $\delta^{15}N$ to determine specific critical years where significant directional shifts in the 1940–2014 chronologies of BAI, $\Delta^{13}C$, and $\delta^{15}N$ occurred. For all further analyses used to examine environmental effects on these proxies of tree growth, photosynthetic physiology and ecosystem N status, we used 1989 as the critical year where this directional shift occurred, which was determined as the average breakpoint of BAI, $\Delta^{13}C$, and $\delta^{15}N$ chronologies (Table 1). We used linear mixed effects (LME) models using the 'nlme' package in R (Pinheiro, Bates, DebRoy, Sarkar, & Team, 2018) with year as the single predictor variable, accounting for temporal autocorrelation with an AR(1,0) structure, and including site as a random factor, to examine temporal trends in BAI, A, g_c, and $\delta^{15}N$ for before (1940–1989) and after (1989–2014) the critical year. We also used breakpoint analysis to identify a critical directional shift that occurred in the iWUE chronology and used the same LME model structure to determine changes in iWUE before and after this year.

Initially, we performed exploratory bootstrapped Pearson's correlations using the R package 'treeclim' (Zang & Biondi, 2015) to examine the relationships between annual, growing season (May–September), and monthly mean, maximum and minimum temperatures, precipitation, and Palmer Drought Severity Index (PDSI) and red spruce tree ring chronologies from 1940 to 2014 (WV Climate Division 4, NOAA, 2017). All chronologies were prewhitened prior to these analyses to remove first-order autocorrelation.

Kendall's rank correlation, a nonparametric correlation analysis (Sokal & Rohlf, 2011), was used to examine the relationships

TABLE 1 Estimated breakpoints (±standard errors) where a directional change in the 1940–2014 chronologies of red spruce basal area increment (BAI), $\Delta^{13}C$, and $\delta^{15}N$ occurred for McGowan Mountain (MCG), Span Oak Run (SOR), and Cranberry Glades (CGL)

Site	BAI	$\Delta^{13}C$	$\delta^{15}N$
MCG	1985 ± 1.8	1990 ± 0.8	1985 ± 2.4
SOR	1993 ± 2.3	1992 ± 0.9	1981 ± 1.8
CGL	1987 ± 2.2	1993 ± 1.0	1994 ± 7.4

At each site, N = 20–25 red spruce trees. The overall breakpoint, defined as the average breakpoint at all three sites and all three proxies, was the year 1989 ± 1.5 years.

between potential explanatory environmental parameters and the dependent variables BAI, $\Delta^{13}C$, A, and g_c over the 1940–2014 chronology, as well as the period 1989–2014. For these analyses, environmental parameters included US emissions of SO_2 and NO_x (Lefohn et al., 1999; EPA, 2015), atmospheric CO_2 concentrations (Keeling et al., 2015), and climate variables (annual, growing season, and monthly mean temperatures, and precipitation) (WV Climate Division 4, NOAA, 2017). We also examined the potential effects of wet deposition of SO_4^{2-} and NO_3^- in precipitation (WV18; NADP, 2015); however, since NADP measurements only partially covered our 1940–2014 chronology, and because the trends of pollutant emissions and trends of atmospheric wet deposition were strongly related (Figure S1a,b), we only used pollutant emissions in these analyses. For $\delta^{15}N$, we used Pearson product-moment correlation to examine the relationships between wood $\delta^{15}N$, US NO_x emissions (EPA, 2015), and NO_3^- deposition (NADP, 2015), as well as the relationships between $\delta^{15}N$ and $\Delta^{13}C$, seasonally integrated A, g_c, and BAI of the red spruce trees.

Although trends in pollutant emissions and CO_2 were clear across the 75-year chronology, changes in climate variables were less clear due to the high interannual variability in temperature and precipitation that occurs in this region of the Central Appalachian Mountains. Thus, to carefully examine the potential influences of temperature and precipitation on the chronologies of BAI, $\Delta^{13}C$, A, and g_c, we first examined the linear trends of annual, growing season, and monthly climate variables to determine if significant changes across 1940–2014 had occurred. Second, we used analysis of covariance (ANCOVA) to determine whether trends in temperature or precipitation were different before and after 1989. Third, we used analysis of variance (ANOVA) to determine if climate variables during the period 1940–1989 were different from 1989 to 2014. Finally, ANCOVA was used to determine whether changes in the responses of BAI, A, and g_c to temperature or precipitation were different before and after 1989.

To examine the influence and interactions of environmental parameters on red spruce BAI from 1940 to 2014 and from 1989 to 2014, we utilized generalized linear mixed models (GLMMs) and model averaging using the R packages 'nlme' and 'MuMIn' (Bartoń, 2017; Pinheiro et al., 2018). Models differing by less than four AICc units, with respect to the best model, were averaged to identify the nature of the relationship between predictor variables and BAI (Fernández-Martínez et al., 2017). The environmental parameters included in this analysis were selected a priori based on their known importance to tree growth and physiology and informed by the results of the initial Kendall's rank correlation and bootsrapped Pearson's correlations. For this analysis, we included atmospheric CO_2, national emissions of SO_2, national emissions of NO_x, and mean April temperatures as predictor variables, exploring all possible combinations of models, including interactions. We also used combinations of other environmental factors in the GLMM averaging, but the four factors listed above consistently provided the best model fit, capturing the greatest variation in BAI while minimizing the unidentified biotic or abiotic contributions to the temporal variation in BAI, determined as an 'unknown' residual effect from the consensus model. In the GLMMs, we accounted for temporal autocorrelation using an AR (1,0) structure, and included environmental parameters as fixed effects, while site was included as a random effect.

The average model was used to identify the relative effect each parameter had on BAI for the 1989–2014 period (Fernández-Martínez et al., 2017). To do this, we first used the average model to predict BAI for a given year. We then ran the model to predict BAI holding a given environmental parameter constant at its respective median value for the region over 1989–2014 (atmospheric CO_2: 371.5 ppm, NO_x emissions: 20.52 million metric tons, SO_2 emissions: 14.04 million metric tons, mean April temperature: 10.08°C), while letting all other parameters change as observed. The difference in slope between BAI predicted from the original model and BAI predicted when holding a particular environmental parameter constant was the contribution of that parameter to predicted BAI. The sensitivity of BAI to each parameter was then determined by dividing the contribution of given parameter to BAI by its own trend over 1989–2014. Finally, we determined the total contribution each environmental parameter had on the total change in BAI over 1989–2014 by multiplying the sensitivity of BAI to each respective environmental parameter by that parameter's total change over 1989–2014 (atmospheric CO_2: +46.8 ppm, NO_x emissions: −13.78 million metric tons, SO_2 emissions: −19.50 million metric tons, mean April temperature: +1.82°C). Standard errors were propagated throughout all calculations using the R package 'propagate' (Spiess, 2017).

Significance was assigned at the $\alpha = 0.05$ level for all analyses. All statistical analyses were performed using JMP software for Macintosh v.12.0 (SAS Institute, Cary NC) or R Version 3.3.3 (R Foundation for Statistical Computing, Vienna, Austria).

3 | RESULTS

3.1 | *Tree ring chronology breakpoints and trends in BAI, $\Delta^{13}C$, and $\delta^{15}N$*

Breakpoint analysis of the 1900–2014 red spruce BAI chronology revealed two distinct breakpoints, with the first at 1941 ± 2.1 years, marking the end of the juvenile growth phase of the red spruce trees (Figure 1). The second breakpoint in BAI was 1988 ± 2.4 years, where a directional shift from declining BAI to

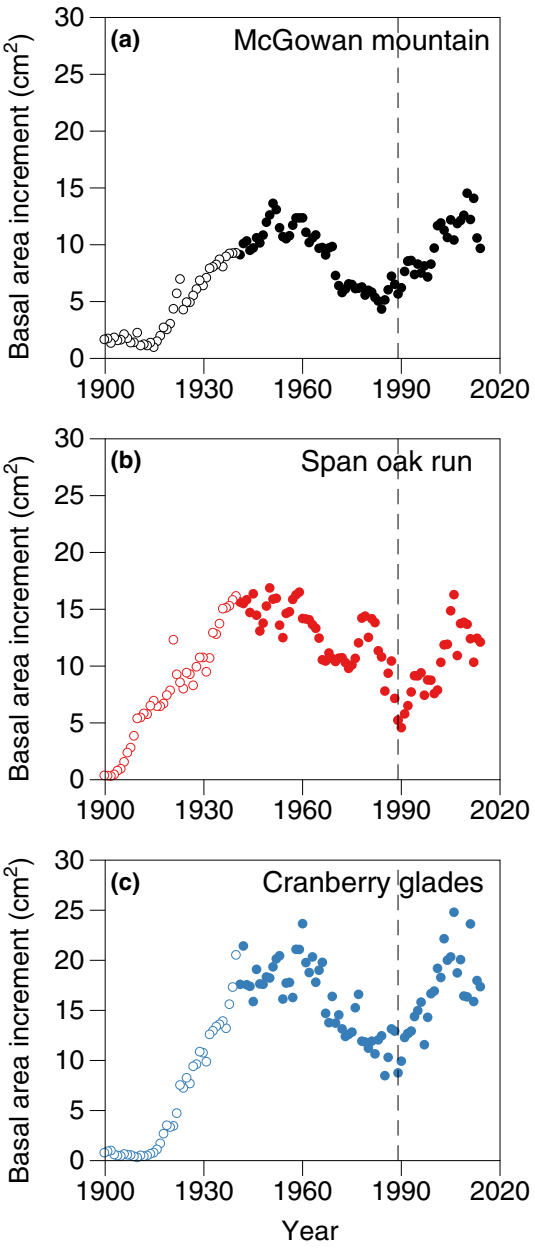

FIGURE 1 Average basal area increment (BAI) of red spruce trees from three forest sites in the Central Appalachian Mountains from 1900 to 2014 (N = 20–25 trees for each site). Open circles indicate the juvenile growth phase after logging in the early 20th Century, whereas closed circles represent the mature growth phase

increasing BAI was observed (Figure 1, Table 1). Breakpoints in 1940–2014 chronologies of $\Delta^{13}C$ and $\delta^{15}N$ exhibit directional changes in the late 20th century that were contemporaneous with those in BAI. Breakpoint analysis for tree ring $\Delta^{13}C$ indicates a directional shift in tree ring $\Delta^{13}C$ signatures at 1991 ± 1.5 years (Figure 2a, Table 1). For tree ring $\delta^{15}N$, breakpoint analysis shows a directional shift in tree ring $\delta^{15}N$ signatures at 1987 ± 3.8 years when averaged over the three sites (Figure 2b, Table 1). One-way ANOVA indicated breakpoint years were not significantly different for a given response variable (BAI, $\Delta^{13}C$, or $\delta^{15}N$) across sites (F = 0.74, p = .52), nor for a given site (MCG, SOR, or CGL) across response variable (F = 0.83, p = .53). Thus, the overall average year where directional changes were observed in the 1940–2014 chronologies of BAI, $\Delta^{13}C$, and $\delta^{15}N$ at all three sites was 1989 ± 1.5 years.

Using 1989 as the overall breakpoint year, red spruce BAI showed a 0.16 cm^2/year decline, or a total reduction of 48.9%, between 1940 and 1989 (p < .0001), but a 0.34 cm^2/year increase, or a total increase of 105.8%, from 1989 to 2014, (p < .0001) (Figure 1). Tree ring $\Delta^{13}C$ signatures declined by 17% between 1940 and 1989 from 20.7 ‰ to 17.7 ‰ (p < .0001), after which $\Delta^{13}C$ signatures increased steadily by 0.070 ‰ each year from 1989 to 2014 (p < .0001) (Figure 2a). Growth rates following the 1989 breakpoint were not different than growth rates during the juvenile period from 1908 to 1941 (ANCOVA, F = 2.92, p = .09; Figure 1). In addition, tree ring $\Delta^{13}C$ signatures for the year 2013 were not different from those for the year 1941 (ANOVA, F = 0.652, p = .47; Figure 2a).

Analysis of the nitrogen isotope composition in whole wood of red spruce tree rings for the 48 years prior to 1989 revealed a mean $\delta^{15}N$ signature of 0.404 ‰, but no trend between 1940 and 1989 (p = .23; Figure 2b). After 1989, however, the $\delta^{15}N$ chronology shows an abrupt, significant depletion in the heavier N isotope in all three red spruce locations as $\delta^{15}N$ progressively declined, on average, by 0.083‰ each year from the mean $\delta^{15}N$ signatures of 0.404 ‰ before 1989 (p < .0001; Figure 2b). The average N concentrations in red spruce tree rings were 32% greater after 1989 (0.059%) compared to wood N concentrations before 1989 (0.045%) (F = 47.37, p < .0001).

3.2 | Changes in environmental factors across the 1940–2014 tree ring chronology

We examined whether there were changes that occurred near 1989 for one or more environmental factors that could possibly explain the observed near simultaneous changes in BAI, tree ring $\Delta^{13}C$ and $\delta^{15}N$ signatures. From 1940 to 1989, SO_2 emissions in the United States averaged 23.13 million metric tons/year, but declined by 0.73 million metric tons/year from 1989 to 2014 (Figure S1a; ANCOVA, F = 129.7, p < .001) (Lefohn et al., 1999; EPA, 2015). From 1940 to 1989, NO_x emissions in the United States increased by 0.92 million metric tons/year (R^2 = .92, p < .01), but declined by 0.56 million metric tons/year from 1989 to 2014 (Figure S1b; R^2 = .91, p < .001) (EPA, 2015). On average, atmospheric CO_2 concentration increased from 311 ppm in 1940 to 397 ppm in 2014, or 1.2 ppm/year (Figure S1c) (Keeling et al., 2015). Moreover, the rate at which atmospheric CO_2 concentration increased was 1.0 ppm/year greater during the 1989–2014 period than during 1940–1989 (ANCOVA, F = 136.5, p < .01) (Keeling et al., 2015).

Mean annual temperatures in this region have increased significantly over the past 75 years by 0.50°C (WV Climate Division 4, NOAA, 2017) (Figure S2a; R^2 = .04, p = .04). In contrast, there were no significant changes in mean annual precipitation (Figure S2b), growing season temperature (Figure S2c), or growing season

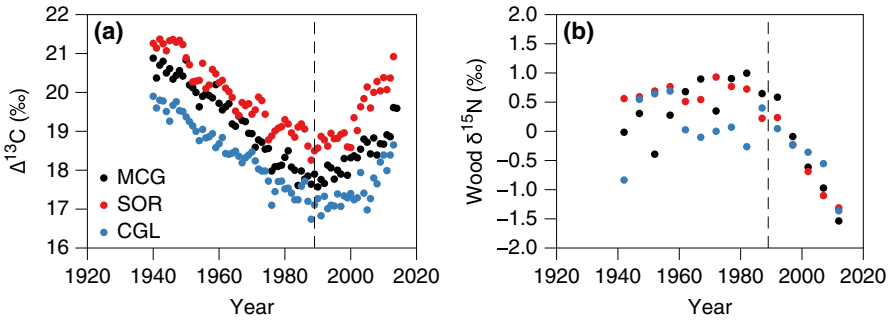

FIGURE 2 (a) Chronology of carbon isotope discrimination, $\Delta^{13}C$, and (b) wood $\delta^{15}N$ for red spruce trees (N = 5 per site) from three forest sites in the central Appalachian Mountains. The $\Delta^{13}C$ chronology in (a) includes 1940–2014, while the $\delta^{15}N$ chronology in (b) includes 1940–2013. The vertical dashed lines in (a) and (b) are at 1989, the average critical year for the region determined via breakpoint analysis where a directional shift in BAI, $\Delta^{13}C$, and $\delta^{15}N$ occurred. The three red spruce forest sites are McGowan Mountain (MCG), Span Oak Run (SOR), and Cranberry Glades (CGL)

precipitation from 1940 to 2014 (Figure S2d) (WV Climate Division 4, NOAA, 2017). With the exception of April mean temperatures, temperature and precipitation in this region have not changed significantly at or around 1989 in a way that could affect BAI, $\Delta^{13}C$, and $\delta^{15}N$. Mean April temperatures increased by 0.06°C/year from 1989 to 2014, but showed no trend prior to 1989 (Figure S1d; ANCOVA, F = 3.90, p = .05), and therefore, mean April temperatures were 0.72°C warmer during 1989–2014 than during 1940–1989 (ANOVA, F = 4.10, p = .05).

3.3 | Assessing environmental influences on seasonally integrated leaf physiology

Chronologies of seasonally integrated leaf physiology modeled using $\Delta^{13}C$ revealed an 11% reduction in A ($p < .0001$; Figure 3a) in red spruce and a 47% reduction in g_c ($p < .0001$; Figure 3b) from 1940 to 1989. From 1989 to 2014, there was a 43% increase in A ($p < .0001$; Figure 3a) and a 67% increase in g_c ($p < .0001$; Figure 3b). Using historical monthly, seasonal, and annual climate variables (WV Climate Division 4, NOAA, 2017), atmospheric CO_2 concentrations (Keeling et al., 2015), and US SO_2 and NO_x emissions (Lefohn et al., 1999; EPA, 2015) to examine environmental influences on A and g_c of red spruce trees, Kendall's rank correlation revealed that A across the entire 1940–2014 chronology was negatively correlated with SO_2 ($\tau = -0.39$, $p < .0001$) and NO_x ($\tau = -0.27$, $p < .0001$) and positively correlated with atmospheric CO_2 ($\tau = 0.20$, $p < .0001$), mean annual temperatures ($\tau = 0.22$, $p < .0001$), and mean April temperatures ($\tau = 0.17$, $p = .0002$). Across the entire chronology, g_c was negatively correlated with NO_x emissions ($\tau = -0.66$, $p < .0001$) and atmospheric CO_2 ($\tau = -0.43$, $p < .0001$) and positively correlated with May temperatures ($\tau = 0.13$, $p < .01$), June temperatures ($\tau = 0.15$, $p < .01$), and June precipitation ($\tau = 0.14$, $p < .01$). Increases in A from 1989 to 2014 are correlated with increases in atmospheric CO_2 ($\tau = 0.73$, $p < .0001$), increases in April temperatures ($\tau = 0.23$, $p < .01$) and reductions in pollutant emissions of SO_2 ($\tau = -0.72$, $p < .0001$) and NO_x ($\tau = -0.69$, $p < .0001$). Furthermore, the temperature response of A was higher for a given April temperature during 1989–2014 than during 1940–1989 (ANCOVA; F = 8.94, p = .003) (Figure 4a). Increases in g_c from 1989 to 2014 are correlated with increases in atmospheric CO_2 ($\tau = 0.63$, $p < .0001$), increases in April temperatures ($\tau = 0.21$, $p < .01$) and May temperatures ($\tau = 0.21$, $p < .01$), as well as reductions in pollutant emissions of SO_2 ($\tau = -0.62$, $p < .0001$) and NO_x ($\tau = -0.59$, $p < .0001$). These environmental factors were the most important influences on A and g_c and complete Kendall's rank correlation analyses are shown in Table S1 for 1940–2014 and in Table 2 for 1989–2014.

In this study, there was a 51% increase in seasonally integrated iWUE across the 75-year red spruce chronology ($p < .0001$; Figure 3c), where iWUE was positively correlated with A (r = .25, p = 0.0002) and negatively correlated with g_c ($r = -.83$, $p < .0001$). There was, however, a breakpoint in iWUE averaged across the three sites at 1995 ± 2.5 years, where iWUE declined 13% after that year ($p < .0001$; Figure 3c). Across the 75-year chronology, BAI of red spruce trees was not correlated with iWUE (p = 0.10), but BAI was positively correlated with A (r = .52, $p < .0001$) and g_c (r = .39, $p < .0001$). Kendall's rank correlation revealed that iWUE during 1940–1995 was positively correlated with atmospheric CO_2 ($\tau = 0.71$, $p < .0001$), NO_x ($\tau = 0.61$, $p < .0001$), mean March temperatures ($\tau = 0.14$, $p = .006$), and mean November temperatures ($\tau = 0.13$, $p = .013$). There was a negative correlation between iWUE during 1940–1995 with June precipitation ($\tau = -0.16$, $p = .002$), mean May temperatures ($\tau = -0.13$, $p = .015$), and mean June temperatures ($\tau = -0.15$, $p = .006$), mean October temperatures ($\tau = -0.13$, $p = .015$), and mean growing season temperatures ($\tau = -0.10$, $p = .05$). After the 1995 breakpoint, after which iWUE declined, Kendall's rank correlation indicated that iWUE was not significantly correlated with any of the environmental factors that we examined.

3.4 | Tree ring nitrogen isotope composition

Reductions in tree ring $\delta^{15}N$ after 1989 were synchronous with increases in tree ring $\Delta^{13}C$ (Figure 5a; MCG, $r = -.98$, p = .005; SOR, $r = -.96$, p = .01; CGL, $r = -.99$, $p < .001$), and strongly

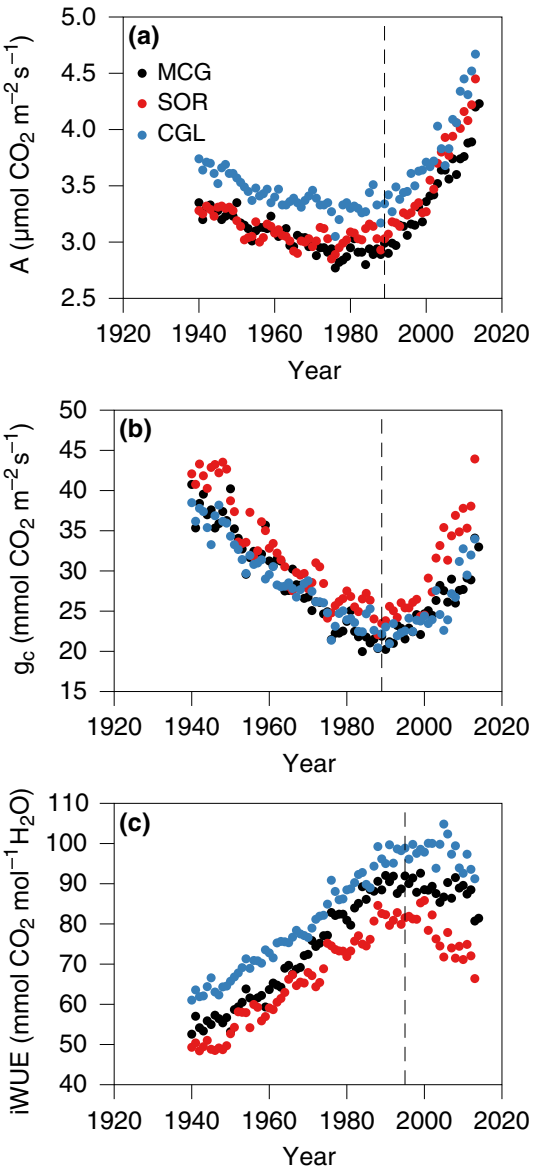

FIGURE 3 (a) Chronology of seasonally integrated photosynthesis modeled using $\Delta^{13}C$ for red spruce trees (N = 5 per site) from three forest sites in the central Appalachian Mountains from 1940 to 2014, (b) seasonally integrated stomatal conductance modeled using $\Delta^{13}C$, and (c) intrinsic water use efficiency (*i*WUE) derived from the chronologies of $\Delta^{13}C$. The vertical dashed lines in (a) and (b) are at 1989, the average critical year for the region determined via breakpoint analysis where a directional shift in BAI, $\Delta^{13}C$, and $\delta^{15}N$ occurred. The vertical dashed line in (c) is at 1995, the critical year where a directional shift in *i*WUE occurred. The three red spruce forest sites are McGowan Mountain (MCG), Span Oak Run (SOR), and Cranberry Glades (CGL)

correlated with increases in A (Figure 5b; MCG, $r = -.99$, $p = .002$; SOR, $r = -.97$, $p = .007$; CGL, $r = -.99$, $p = .002$) and g_c (Figure 5c; MCG, $r = -.98$, $p = .004$; SOR, $r = -.95$, $p = .01$; CGL, $r = -.99$, $p < .001$) at each red spruce site, although the correlations between tree ring $\delta^{15}N$ and red spruce growth were more variable (Figure 5d; MCG $r = -.87$, $p = .056$; SOR $r = -.93$, $p = .02$; CGL $r = -.60$, $p = .28$). The proximate reduction of $\delta^{15}N$ after 1989 was positively correlated with the decline in national emissions of NO_x ($r = .92$, $p < .0001$; Figure S3a) and local wet deposition of NO_3^- ($r = .86$, $p < .0001$; Figure S3b).

3.5 | Assessing environmental influences on BAI

We first used bootstrapped Pearson's correlations to explore the relationships between current year ring width indices at each red spruce location and monthly mean temperature and precipitation of the current and previous year (Figure S4, Table S2) (WV Climate Division 4, NOAA, 2017). We found no significant correlations between radial growth and these climate variables, except for a weak positive correlation with the previous year's July precipitation at one red spruce location (SOR) ($r = .18$, $p < .05$). There were no significant correlations between tree radial growth and maximum monthly temperature, minimum monthly temperature, or PDSI at our red spruce study locations (Table S2).

Kendall's rank correlation revealed that BAI of red spruce trees from 1940 to 2014 declined as atmospheric CO_2 increased ($\tau = -0.14$, $p = .002$), as pollutant emissions of NO_x ($\tau = -0.34$, $p < .0001$) and SO_2 increased ($\tau = -0.12$, $p = .01$) (Table S1). GLMMs identified only a negative relationship between NO_x emissions and BAI over 1940–2014 ($p < .001$, -0.353 ± 0.05 slope estimate ± standard error), with no other models with a ΔAICc < 4. Kendall's rank correlation showed increases in BAI from 1989 to 2014 were correlated with increases in atmospheric CO_2 ($\tau = 0.41$, $p < .0001$), increases in April temperatures ($\tau = 0.26$, $p < .001$) and reductions in pollutant emissions of SO_2 ($\tau = -0.42$, $p < .0001$) and NO_x ($\tau = -0.36$, $p < .0001$). Additionally, the temperature response of BAI to April temperatures was greater during 1989–2014 than during 1940–1989 (ANCOVA; $F = 6.96$, $p = .009$) (Figure 4b).

In order to specifically examine the recent increases in BAI from 1989 to 2014, model averaging of the best models (ΔAICc < 4 from the best model; hereafter referred to as 'average model') determined by GLMMs indicated the importance of mean April temperatures, a negative interaction between SO_2 and NO_x emissions, a positive interaction between atmospheric CO_2 and SO_2 emissions, and a positive interaction between atmospheric CO_2 and NO_x emissions (Table S3). We found that over the 1989–2014 period the average model predicts an increase in BAI of 0.29 ± 0.02 cm^2/year ($t = 15.60$, $p < .001$) (Figure 6a), in close agreement with observed BAI ($R^2 = .85$, $p < .001$) (Figure S5). Of the 0.29 cm^2/year increase in BAI, increasing atmospheric CO_2 contributed to a 0.17 ± 0.02 cm^2/year increase in BAI ($t = 96.05$, $p < .01$). Reductions in national emissions of SO_2 contributed to a 0.11 ± 0.02 cm^2/year increase in BAI ($t = 17.18$, $p < .01$), while decreasing emissions of NO_x reduced BAI by 0.06 ± 0.02 cm^2/year ($t = -7.68$, $p < .01$). Higher April temperatures contributed to a small increase in BAI by 0.04 ± 0.03 cm^2/year ($t = 3.65$, $p < .01$) (Figure 6a). Unknown contributions due to unidentified biotic or abiotic factors were calculated as the difference between the observed change and all known contributions and accounted for 0.04 ± 0.05 cm^2/year ($t = 1.08$, $p = .28$). Sensitivity

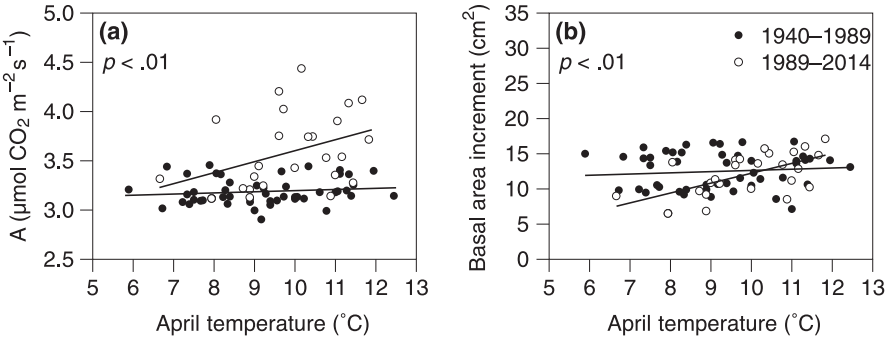

FIGURE 4 (a) Relationships between seasonally integrated photosynthesis and (b) basal area increment with mean April temperatures before and after 1989. ANCOVA was used to determine if the response of seasonally integrated photosynthesis or basal area increment to April temperatures were different before and after 1989, the average critical year for the region determined via breakpoint analysis where a directional shift in BAI, $\Delta^{13}C$, and $\delta^{15}N$ occurred. Climate data are from West Virginia Division 4, which is the region that contains the three red spruce stands in this study (WV Climate Division 4, NOAA, 2017)

analysis of GLMM results revealed that over 1989–2014 average BAI was the most sensitive to increases in April temperatures and reductions in SO_2 emissions, followed by reductions in NO_x, and increases in atmospheric CO_2 (Table 3).

These results indicate that increasing atmospheric CO_2 was responsible for the largest change in basal area of the red spruce trees, producing a 4.38 ± 0.6 cm^2 increase between 1989 and 2014. Reductions in national SO_2 emissions were the second most important factor, contributing to a 2.96 ± 0.52 cm^2 increase in basal area (Figure 6b). Lastly, reductions in national emissions of NO_x negatively impacted basal area by −1.70 ± 0.52 cm^2, while increases in mean April temperatures contributed positively to a 1.01 ± 0.80 cm^2 increase in basal area (Figure 6b).

TABLE 2 Kendall's rank correlation coefficients (τ) between environmental parameters and the regional chronologies from 1989 to 2014 of basal area increment (BAI), $\Delta^{13}C$, seasonally integrated net photosynthesis (*A*), and seasonally integrated stomatal conductance (g_c) of red spruce trees from three locations in the central Appalachian Mountains

Environmental parameter	BAI	$\Delta^{13}C$	*A*	g_c
NO_x	−0.364***	−0.326***	−0.689***	−0.594***
SO_2	−0.422***	−0.338***	−0.718***	−0.618***
Atmospheric CO_2	0.414***	0.343***	0.727***	0.625***
MGT			0.207	0.193
January temperature			−0.203	−0.215*
February temperature			−0.175	−0.171
April temperature	0.263**		0.233*	0.210*
May temperature			0.190	0.211*
February precipitation	−0.154		−0.186	
March precipitation			−0.165	
December precipitation			0.167	0.157

Environmental parameters included national SO_2 and NO_x emissions (Lefohn et al., 1999; EPA, 2015), atmospheric CO_2 concentrations (Keeling et al., 2015), and monthly, growing season, and annual precipitation and temperatures (WV Climate Division 4, NOAA, 2017). τ is shown for significant correlations only, and *$p < .01$, **$p < .001$, while ***$p < .0001$.

4 | DISCUSSION

A synchronous change in three tree ring proxy indicators, BAI, $\Delta^{13}C$, and $\delta^{15}N$, identified 1989 as the average year that three forest stands of red spruce trees, spanning 100 km in the Central Appalachian Mountains, began a 25 year period of accelerated tree growth (Table 1). Prior to 1989, there was a 49 year period of declining tree growth, characteristic of reduced growth of red spruce trees exposed to high levels of acidic air pollution and deposition in the eastern United States. (Cook, Johnson, & Blasing, 1987; Eager & Adams, 1992; Johnson, Cook, & Siccama, 1988). Our observations of recent increases in growth of red spruce trees are similar to observations of increased growth of red spruce in the northeastern United States (Engel et al., 2016) and other tree species in the eastern United States (Fang et al., 2014; Johnson & Abrams, 2009; McMahon et al., 2010; Thomas et al., 2013). In our study, GLMM model averaging used to examine the environmental influences on growth of red spruce from 1989 to 2014 indicated recovery from reduced acidic air pollution, a fertilization effect of increased atmospheric CO_2, and a positive influence of early spring temperatures, thus highlighting the importance of multiple environmental factors on the proximate increases in red spruce tree growth in the Central Appalachian Mountains.

Since the Clean Air Act of 1970 and subsequent amendments, pollutant emissions in the United States have dropped considerably. From 1940 to 1989, SO_2 emissions averaged 23.13 million metric tons/year, but declined by 0.73 million metric tons/year from 1989 to 2014 (Figure S1a) (Lefohn et al., 1999; EPA, 2015). Kendall's rank correlation placed the decline in SO_2 emissions as the topmost environmental factor contributing to the observed growth increases in red spruce trees since 1989 (Table 2). GLMM model averaging also

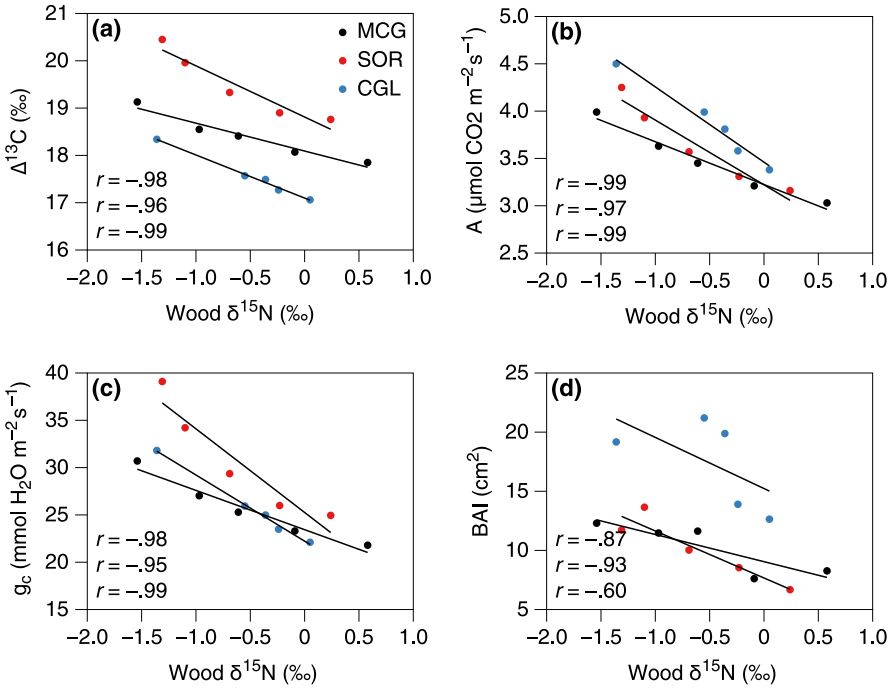

FIGURE 5 (a) Relationships between carbon isotope discrimination, (b) seasonally integrated photosynthesis, (c) seasonally integrated stomatal conductance, and (d) basal area increment with wood $\delta^{15}N$ at each red spruce site ($N = 5$ trees per site) from 1989 to 2013. In each panel, correlation coefficients are from top to bottom, McGowan Mountain (MCG), Span Oak Run (SOR), and Cranberry Glades (CGL)

pointed to a strong effect of decreasing SO_2 emissions on tree growth across 1989–2014, as well as a high sensitivity to these pollutant reductions (Figure 6, Table 3). The changes in the red spruce $\Delta^{13}C$ chronology, a proxy indicator for photosynthetic physiology, further support recovery of these trees from acid pollution. The decrease in $\Delta^{13}C$ in the red spruce tree rings from 1940 to 1989, corresponding to reductions in A and g_c, has been shown in many studies examining the effects of acidic sulfur pollution on the C isotope signatures of trees (Boettger, Haupt, Friedrich, & Waterhouse, 2014; Kwak et al., 2016; Rinne, Loader, Switsur, Treydte, & Waterhouse, 2010; Santruckova, Santrucek, Setlik, Svoboda, & Kopacek, 2007; Savard, Bégin, Parent, Smirnoff, & Marion, 2004), including species from the eastern United States (Li et al., 2010; Thomas et al., 2013). The increase in $\Delta^{13}C$, corresponding to increases in A and g_c, that we observed after 1989 as SO_2 emissions declined, has also been found in studies as a function of decreasing pollution (Boettger et al., 2014; Li et al., 2010; Thomas et al., 2013), and is opposite from observations of reduced tree ring $\Delta^{13}C$ with increased tree height or as trees get older (Brienen et al., 2017; McDowell, Bond, Dickman, & Ryan, 2011). Thus, our data are consistent with the hypothesis that reductions in acidic air pollution and deposition from the historically high totals in the 1970s reached a critical level around 1989 that red spruce trees were better able to tolerate, thereby beginning the recovery of tree growth and photosynthetic physiology of red spruce trees in the Central Appalachian Mountains that has persisted for 25 years as pollution levels continued to decline.

Our study suggests that increases in growth and A after 1989 were likely enhanced by increases in atmospheric CO_2 concentrations, which have increased substantially over the last 75 years and have increased by *ca.* 13% from 1989 to 2014 (Keeling et al., 2015). Although numerous experiments using large square-wave increases in CO_2, such as FACE experiments, often show increased tree growth (Norby et al., 2005), an effect of increasing CO_2 on growth is rarely observed in tree ring studies, possibly because the annual step changes in CO_2 are small and any changes in growth are masked by other environmental factors positively or negatively contributing to growth. In our study, both Kendall's rank correlation and GLMM model averaging indicate strong effects of increasing CO_2 on red spruce growth from 1989 to 2014 (Figure 6). In addition, if A is considered a diffusive process, where $A = (C_a – C_i)*g_c$, then the 43% increase in A of red spruce trees after 1989 is likely produced by the combination of the 13% increase in C_a and the 67% increase in g_c as acidic pollution declines. Our data suggesting a CO_2 enhancement of growth and A of red spruce trees since 1989 are consistent with flux tower observations of increased forest productivity from 23 forest sites in the United States and Europe from 1995 to 2011, where increases in atmospheric CO_2 were shown to stimulate GPP and NEP (Fernández-Martínez et al., 2017).

Both SO_4^{2-} deposition and elevated CO_2 reduce g_c experimentally (Ainsworth & Rogers, 2007; Borer, Schaberg, & DeHayes, 2005) and, thus, the combined effects of acid deposition and increasing atmospheric CO_2 are likely responsible for the 47% decline in g_c of red spruce trees from 1940 to 1989. If we assume that the increase in g_c after 1989 represents a complete recovery from acid deposition, then the 15% reduction in g_c from 1940 to 2014 reflects only the effect of increasing CO_2 on g_c of the red spruce trees (Figure S6a) and is more in line with observed reductions in g_c per ppm CO_2 increase from elevated CO_2 experiments using trees (Ainsworth & Rogers, 2007). Under this assumption, our data indicate that acidic air pollution is a 3.7× greater forcing factor on g_c of red spruce trees than increasing CO_2 (Figure S6a). Numerous experiments, as well as

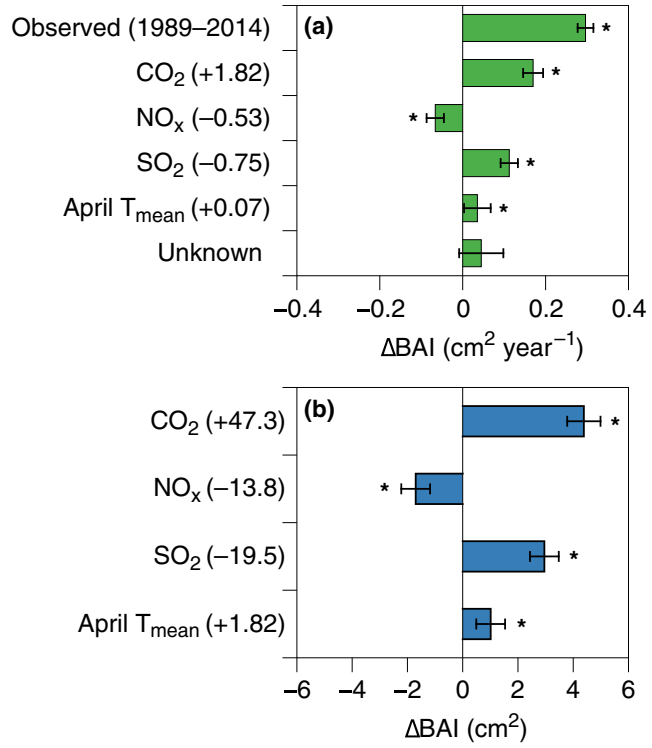

FIGURE 6 (a) Contribution of atmospheric CO_2, NO_x emissions, SO_2 emissions, and mean April temperatures to the change in BAI each year predicted by the GLMM average model for 1989–2014, and (b) the contribution of CO_2, NO_x emissions, SO_2 emissions, and mean April temperatures to the total change in BAI over 1989–2014. Numbers in brackets indicate the direction and magnitude of changes in environmental parameters. Numbers in brackets in panel (a) represent the trend in each respective environmental parameter over 1989–2014, while numbers in brackets in panel (b) represent the total change in each respective environmental parameter over 1989–2014. Units for CO_2 and April T_{mean} are ppm and °C, respectively, while units for NO_x and SO_2 are 10^6 metric tons. Unknown contributions in (a) were calculated as the difference between the observed change and all known contributions. Models with ΔAICc < 4 were included in the average model (see Table S3 for model structure). Asterisks (*) indicate significance at the $\alpha = 0.05$ level

dendroisotopic studies, have shown that *i*WUE, the ratio of *A* to stomatal conductance of water, of many plants is improved as a result of a combination of increasing CO_2 stimulating *A* and causing partial stomatal closure (Ainsworth & Rogers, 2007; Franks et al., 2013; Keenan et al., 2013; Knauer et al., 2016), and this has been hypothesized to be an important mechanism leading to increased forest productivity. Over the 1940–2014 tree ring chronology, *i*WUE of red spruce trees increased 51%, or +0.68% per year, as *A* increased by 27% and g_c declined by 15% from 1940 to 2014. If we use the Ball–Berry model to predict the theoretical change in *i*WUE if impacted by changes in CO_2 alone, using a constant C_i/C_a ratio of 0.72 (mean at 1940), then *i*WUE increases by 30% over the tree ring chronology (Figure S6b), tracking the increase in atmospheric CO_2 (Knauer et al., 2016). If we model *i*WUE using the decline in g_c attributed to increasing CO_2 for red spruce trees in this study

TABLE 3 Mean sensitivity (±standard errors) of BAI to each environmental parameter determined to be significant by the average model for the 1989 to 2014 period

Factor	Sensitivity
Atmospheric CO_2 (ppm)	0.093 ± 0.013
SO_2 emissions (10^6 metric tons)	−0.152 ± 0.029
NO_x emissions (10^6 metric tons)	0.123 ± 0.040
April temperature (°C)	0.556 ± 0.521

Sensitivities are defined as the change in BAI (cm^2) to a one-unit change for each of the environmental factors listed and were determined by dividing the contribution of each factor to BAI by the respective trend of each factor over 1989–2014. Units for environmental factors are in parentheses.

(−15%, Figure S6a) and an increase in *A* that is predicted from CO_2 enrichment studies using trees (Ainsworth & Rogers, 2007), scaled over the range of CO_2 during our study (9.3% increase in *A* from 1940 to 1989), then *i*WUE increases by 41% over the tree ring chronology (Figure S6b). Both of these examples, point to the much greater sensitivity of g_c to acidic sulfur pollution than to CO_2 and the subsequent role of pollution in the observed increases of *i*WUE. In addition, several analyses have observed that increases in *i*WUE do not always translate into greater tree growth (Lévesque, Siegwolf, Saurer, Eilmann, & Rigling, 2014; Peñuelas, Canadell, & Ogaya, 2011; Silva, Anand, & Leithead, 2010). In our study, BAI declined 48.9% from 1940 to 1989 as *i*WUE increased 67.2%, from 1989 to 1995, BAI increased 63.6% as *i*WUE increased 0.6%, and from 1995 to 2014, BAI increased 37.4% as *i*WUE decreased 9.8%. Thus, our study agrees with these analyses that *i*WUE is a poor predictor of tree growth, especially in mesic environments, such as our red spruce forest locations in the Central Appalachian Mountains.

From 1940 to 1989, NO_x emissions increased by 0.92 million metric tons/year, but declined by 0.56 million metric tons/year from 1989 to 2014 (EPA, 2015). GLMM model averaging indicated that tree growth of red spruce across 1989–2014 was negatively impacted by reductions in NO_x emissions after 1989 (Figure 6). This result was surprising given that Kendall's rank correlation identified strong negative correlations between NO_x emissions and BAI, $\Delta^{13}C$, *A*, and g_c after 1989 (Table 2), as well as across the entire 1940–2014 chronology (Table S1). These contradictory results highlight the uncertainty associated with the effects of N deposition on tree growth since N deposition may act as a source of soil acidity and negatively impact tree growth or may act as a fertilizer source of N and positively impact tree growth (Jennings et al., 2016; Thomas, Canham, Weathers, & Goodale, 2010).

The negative correlations between tree ring $\delta^{15}N$ and BAI, $\Delta^{13}C$, *A*, and g_c after 1989 add to the difficulty of interpreting the NO_x emissions results from our GLMM model averaging, as our $\delta^{15}N$ chronology would suggest red spruce tree growth and photosynthesis increased as ecosystem N availability declined. However, even with the dramatic declines in N deposition in this region, an examination of N cycling at these three red spruce forest sites suggests that these ecosystems are not strongly N-limited (Smith et al., 2016).

Given the close relationship between tree ring $\delta^{15}N$ and declines in national emissions of NO_x and local wet deposition of NO_3^- (Figure S3), one may hypothesize that the $\delta^{15}N$ signatures in the red spruce tree ring chronologies reflect changes in the $\delta^{15}N$ signatures of pollutant sources, since NO_3^- produced from fossil fuel combustion is enriched in ^{15}N relative to biogenic sources (Felix, Elliott, & Shaw, 2012). However, the evidence that tree ring $\delta^{15}N$ reflects $\delta^{15}N$ from fossil fuel sources is limited (Gerhart & McLauchlan, 2014), and although the source $\delta^{15}N$ signature of N deposition over the tree ring chronology is unknown at our locations, our data do not support this hypothesis given the constant wood $\delta^{15}N$ prior to 1989 when NO_x emissions were increasing dramatically (Figure 2b, Figure S1).

An alternative hypothesis is that $\delta^{15}N$ in plant tissues, including tree rings, reflects ecosystem N supply relative to demand, where a more open N cycle, defined as a scenario where N supply exceeds plant demand, typically results in greater rates of net nitrate production (a process that strongly fractionates against ^{15}N) followed by the loss of isotopically light nitrate by leaching and/or denitrification (Gerhart & McLauchlan, 2014). The loss of ^{15}N-depleted nitrate enriches the residual pool of plant available N that, in turn, leads to elevated values of $\delta^{15}N$ in plant tissue (Pardo, Hemond, Montoya, Fahey, & Siccama, 2002). Following this line of reasoning, the red spruce tree ring $\delta^{15}N$ chronology between 1940 and 1989 may reflect a more open N cycle resulting from declining tree growth rates and, therefore, a reduced plant demand for N by red spruce trees. Likewise, the decrease in wood $\delta^{15}N$ after 1989 may have resulted from a tighter, more closed N cycle, as increased tree growth created a greater demand for N during a time of reductions in N deposition (Figure 1, Figure S1b). In addition, N concentrations in wood were 32% greater after 1989 compared to before 1989, and this, along with greater tree growth, further suggests that plant N uptake and retention increased after 1989. Our $\delta^{15}N$ data reflect observations of declining tree ring $\delta^{15}N$ signatures across the continental United States in recent decades (Elmore, Nelson, & Craine, 2016; McLauchlan et al., 2017) and support the patterns found in the European NITREX studies where experimental removal of N deposition from throughfall led to rapid ecosystem recovery and a more closed N cycle as losses of gaseous N through denitrification and NO_3^- leaching declined (Bredemeier et al., 1998; Corre & Lamersdorf, 2004). Thus, the $\delta^{15}N$ chronology found in these red spruce trees has broad implications for regional forest ecosystem recovery to pollution, as well as increased water quality and fewer occurrences of eutrophication, since it is likely that less N is lost into stream runoff as N inputs from pollution decline, as has been shown in this region by Eshleman, Sabo, and Kline (2013).

Changes in historical climate were the least influential environmental variables affecting BAI, $\Delta^{13}C$, and seasonally integrated A and g_c of red spruce trees after 1989, possibly due to the high interannual variability in temperature and precipitation in the Central Appalachian region (WV Climate Division 4, NOAA, 2017). Precipitation at our study locations did not significantly change over the study period. Precipitation was not different before and after 1989 (Figure S2b,d), and thus, was not identified by either Kendall's rank correlation or GLMMs as having an influence on BAI, $\Delta^{13}C$, A, or g_c from 1989 to 2014. Our results are contrary to Levesque, Andreu-Hayles, and Pederson (2017), who concluded that increasing water availability after 1984, and not increases in CO_2 or reductions in acid pollution, has been the primary factor driving increases in BAI, A, and g_c of two broadleaf species, *Quercus rubra* and *Liriodendron tulipifera*, at Black Rock, NY, where annual precipitation increased 4% and growing season precipitation increased 19% during 1984–2014 compared to 1950–1983 (PRISM Climate Group, 2004).

On the other hand, mean annual temperatures in this Central Appalachian region have significantly increased by 0.50°C over the past 75 years, which was largely contributed to by a 0.72°C increase in mean April temperatures during 1989–2014 compared to 1940–1989 (WV Climate Division 4, NOAA, 2017). Our tree ring data point to changes in early spring phenology of red spruce trees due to these warmer temperatures after 1989 that are manifested as greater tree growth. First, Kendall's rank correlation identified a strong positive correlation between mean April temperatures and BAI, A, and g_c of red spruce trees during 1989–2014. Second, the GLMM average model indicated a main effect of April temperatures on BAI of red spruce during 1989–2014 that contributed to tree growth increases, and showed a very high sensitivity, suggesting that even small changes in spring temperatures can affect tree growth. Finally, ANCOVA indicated that greater mean April temperatures after 1989 translated to greater seasonally integrated A and, a subtle, but significant, increase in *BAI* of red spruce trees compared to 1940–1989 (Figure 4). Our observations of an accelerated early spring phenology of red spruce trees due to higher spring temperatures are similar to observations of other tree species globally (Black et al., 2000; Piao, Friedlingstein, Ciais, Viovy, & Demarty, 2007), as well as in the eastern United States (Dragoni et al., 2011; Elmore et al., 2016; Richardson et al., 2009).

A large number of elevated CO_2 experiments have generated critical information on how the C cycle is changing in the world's ecosystems (Long, Ainsworth, Rogers, & Ort, 2004; Norby et al., 2005). However, isolating the effects of increasing CO_2 on tree growth in forest ecosystems has been difficult to confirm due to the small annual step changes in CO_2 and the myriad of interacting environmental factors known to affect whole-tree growth over multidecadal time spans (Hyvönen et al., 2007; Luo & Reynolds, 1999). This study not only provides evidence for increasing CO_2 having a positive effect on tree growth but also indicates a broad range of complexity as red spruce forest ecosystems recover from decades of acidic air pollution and the realization that none of the environmental factors that are examined here act in isolation. Although declines in acidic air pollution and increases in atmospheric CO_2 have contributed to increases in red spruce tree growth after 1989, climate change during the early spring also has occurred, which in turn, positively affected the growth of the red spruce trees. It remains unclear how long the increases in growth of these red spruce stands will be sustained. Plant available N will likely be important to maintain this increase in productivity (Luo et al., 2004) and, despite evidence of

increased N uptake and retention by the red spruce trees, N inputs from anthropogenic sources are clearly declining. Although the purpose of our study was to examine the timing and physiological basis of recent growth by red spruce trees in the Central Appalachian Mountains, a simple scaling exercise using our tree growth data, red spruce allometry (Siccama et al., 1994; Whittaker, Bormann, Likens, & Siccama, 1974), and forest inventory biomass data (Kellndorfer et al., 2012) coupled with forest land cover estimates (Homer et al., 2015) (Figure S7) suggests the carbon sink in the northeastern temperate forest could have been reduced by as much as 0.79 Pg C since 1940 due to acid deposition (Table S4), or roughly equivalent to 12% of anthropogenic growth in global atmospheric C in 2016 (Le Quéré et al., 2018), if all species responded the same as red spruce trees. While this back of the envelope estimate clearly needs refinement using a range of species sensitivities to acidic pollution, our assessment suggests that a significant portion of the increases in the temperate forest carbon sink in the United States observed by Pan et al. (2011) could be explained by recovery of trees from decades of acid deposition. This highlights the necessity to better quantify the influence of acidic air pollution on forest ecosystems globally in order to accurately resolve the contribution of forests to the global carbon cycle.

ACKNOWLEDGEMENTS

We thank Stephanie Connolly and Kent Karriker at the Monongahela National Forest for access to the red spruce forest sites; Dr. Dave Nelson and Robin Paulman at the Central Appalachian Stable Isotope Facility (UMCES – Appalachian Laboratory); Dr. Kenneth Smith, Leigh Ann Scholtz, Benjamin Russell, and Dr. Chris Walter for assistance in the field and lab; Dr. Eddie Brzostek, Dr. William Peterjohn, and three anonymous reviewers for thoughtful and constructive comments on the manuscript. This research was funded by the National Science Foundation (Award 1354689).

ORCID

Justin M. Mathias http://orcid.org/0000-0001-5470-4167

REFERENCES

Ainsworth, E. A., & Rogers, A. (2007). The response of photosynthesis and stomatal conductance to rising [CO_2]: Mechanisms and environmental interactions. *Plant, Cell & Environment*, *30*, 258–270. https://doi.org/10.1111/j.1365-3040.2007.01641.x

Anderson-Teixeira, K. J., Miller, A. D., Mohan, J. E., Hudiburg, T. W., Duval, B. D., & DeLucia, E. H. (2013). Altered dynamics of forest recovery under a changing climate. *Global Change Biology*, *19*, 2001–2021. https://doi.org/10.1111/gcb.12194

Bartoń, K. (2017). *MuMIn: Multi-model inference*. R package version 1.40.0.

Belmecheri, S., Maxwell, R. S., Taylor, A. H., Davis, K. J., Freeman, K. H., & Munger, W. J. (2014). Tree-ring $\delta^{13}C$ tracks flux tower ecosystem productivity estimates in a NE temperate forest. *Environmental Research Letters*, *9*, 74011. https://doi.org/10.1088/1748-9326/9/7/074011

Black, T. A., Chen, W. J., Barr, A. G., Arain, M. A., Chen, Z., Nesic, Z., … Yang, P. C. (2000). Increased carbon sequestration by a boreal deciduous forest in years with a warm spring. *Geophysical Research Letters*, *27*, 1271–1274. https://doi.org/10.1029/1999GL011234

Boettger, T., Haupt, M., Friedrich, M., & Waterhouse, J. S. (2014). Reduced climate sensitivity of carbon, oxygen and hydrogen stable isotope ratios in tree-ring cellulose of silver fir (*Abies alba* Mill.) influenced by background SO_2 in Franconia (Germany, Central Europe). *Environmental Pollution*, *185*, 281–294. https://doi.org/10.1016/j.envpol.2013.10.030

Boisvenue, C., & Running, S. W. (2006). Impacts of climate change on natural forest productivity - evidence since the middle of the 20th century. *Global Change Biology*, *12*, 862–882. https://doi.org/10.1111/j.1365-2486.2006.01134.x

Borer, C. H., Schaberg, P. G., & DeHayes, D. H. (2005). Acidic mist reduces foliar membrane-associated calcium and impairs stomatal responsiveness in red spruce. *Tree Physiology*, *25*, 673–680. https://doi.org/10.1093/treephys/25.6.673

Bredemeier, M., Blanck, K., Xu, Y. J., Tietema, A., Boxman, A. W., Emmett, B., … Wright, R. F. (1998). Input-output budgets at the NITREX sites. *Forest Ecology and Management*, *101*, 57–64. https://doi.org/10.1016/S0378-1127(97)00125-4

Brienen, R. J. W., Gloor, E., Clerici, S., Newton, R., Arppe, L., Boom, A., … Helle, G. (2017). Tree height strongly affects estimates of water-use efficiency responses to climate and CO_2 using isotopes. *Nature Communications*, *8*, 288. https://doi.org/10.1038/s41467-017-00225-z

Bunn, A., Korpela, M., Biondi, F., Campelo, F., Mérian, P., Qeadan, F., … Schulz, M. (2015). *Dendrochronology program library in R*. R package version 1.6.3.

Burnham, M. B., McNeil, B. E., Adams, M. B., & Peterjohn, W. T. (2016). The response of tree ring $\delta^{15}N$ to whole-watershed urea fertilization at the Fernow Experimental Forest, WV. *Biogeochemistry*, *130*, 133–145. https://doi.org/10.1007/s10533-016-0248-y

Caspersen, J. P., Pacala, S. W., Jenkins, J. C., Hurtt, G. C., Moorcroft, P. R., & Birdsey, R. A. (2000). Contributions of land-use history to carbon accumulation in U.S. forests. *Science*, *290*, 1148–1151. https://doi.org/10.1126/science.290.5494.1148

Choi, W.-J., Lee, S.-M., Chang, S. X., & Ro, H. (2005). Variations of $\delta^{13}C$ AND $\delta^{15}N$ in *Pinus densiflora* tree-rings and their relationship to environmental changes in Eastern Korea. *Water, Air, and Soil Pollution*, *164*, 173–187. https://doi.org/10.1007/s11270-005-2253-y

Cook, E. R., Johnson, A. H., & Blasing, T. J. (1987). Forest decline: Modeling the effect of climate in tree rings. *Tree Physiology*, *3*, 27–40. https://doi.org/10.1093/treephys/3.1.27

Corre, M. D., & Lamersdorf, N. P. (2004). Reversal of nitrogen saturation after long-term deposition reduction: Impact on soil nitrogen cycling. *Ecology*, *85*, 3090–3104. https://doi.org/10.1890/03-0423

Craine, J. M., Brookshire, E. N. J., Cramer, M. D., Hasselquist, N. J., Koba, K., Marin-Spiotta, E., & Wang, L. (2015). Ecological interpretations of nitrogen isotope ratios of terrestrial plants and soils. *Plant and Soil*, *396*, 1–26. https://doi.org/10.1007/s11104-015-2542-1

Craine, J. M., Elmore, A. J., Aidar, M. P., Bustamante, M., Dawson, T. E., Hobbie, E. A., … Wright, I. J. (2009). Global patterns of foliar nitrogen isotopes and their relationships with climate, mycorrhizal fungi, foliar nutrient concentrations, and nitrogen availability. *New Phytologist*, *183*, 980–992. https://doi.org/10.1111/j.1469-8137.2009.02917.x

Dragoni, D., Schmid, H. P., Wayson, C. A., Potter, H., Grimmond, C. S. B., & Randolph, J. C. (2011). Evidence of increased net ecosystem productivity associated with a longer vegetated season in a deciduous forest in south-central Indiana, USA. *Global Change Biology*, *17*, 886–897. https://doi.org/10.1111/j.1365-2486.2010.02281.x

Driscoll, C. T., Lawrence, G. B., Bulger, A. J., Butler, T. J., Cronan, C. S., Eagar, C., … Weathers, K. C. (2001). Acidic deposition in the Northeastern United States: Sources and inputs, ecosystem effects, and management strategies. *BioScience*, *51*, 180. https://doi.org/10.1641/0006-3568(2001)051[0180:ADITNU]2.0.CO;2

Dye, A., Barker Plotkin, A., Bishop, D., Pederson, N., Poulter, B., & Hessl, A. (2016). Comparing tree-ring and permanent plot estimates of aboveground net primary production in three eastern U.S. forests. *Ecosphere*, *7*, e01454. https://doi.org/10.1002/ecs2.1454

Eager, C., & Adams, M. B. (1992). *Ecology and Decline of Red Spruce in the Eastern United States. Ecological Studies 96*. New York, NY: Springer-Verlag. https://doi.org/10.1007/978-1-4612-2906-3

Elliott, E. M., Kendall, C., Wankel, S. D., Burns, D. A., Boyer, E. W., Harlin, K., … Butler, T. J. (2007). Nitrogen isotopes as indicators of NO_x source contributions to atmospheric nitrate deposition across the Midwestern and Northeastern United States. *Environmental Science & Technology*, *41*, 7661–7667. https://doi.org/10.1021/es070898t

Elmore, A. J., Nelson, D. M., & Craine, J. M. (2016). Earlier springs are causing reduced nitrogen availability in North American eastern deciduous forests. *Nature Plants*, *2*, 1–5.

Engel, B. J., Schaberg, P. G., Hawley, G. J., Rayback, S. A., Pontius, J., Kosiba, A. M., & Miller, E. K. (2016). Assessing relationships between red spruce radial growth and pollution critical load exceedance values. *Forest Ecology and Management*, *359*, 83–91. https://doi.org/10.1016/j.foreco.2015.09.029

Eshleman, K. N., Sabo, R. D., & Kline, K. M. (2013). Surface water quality is improving due to declining atmospheric N deposition. *Environmental Science and Technology*, *47*, 12193–12200. https://doi.org/10.1021/es4028748

Evans, R. D. (2001). Physiological mechanisms influencing plant nitrogen isotope composition. *Trends in Plant Science*, *6*, 121–126. https://doi.org/10.1016/S1360-1385(01)01889-1

Evans, R. D. (2007). Soil nitrogen isotope composition. In R. Michener & K. Lajtha (Eds.), *Stable isotopes in ecology and environmental science* (pp. 83–98). Hoboken, NJ: Wiley-Blackwell.

Fang, J., Kato, T., Guo, Z., Yang, Y., Hu, H., Shen, H., … Houghton, R. A. (2014). Evidence for environmentally enhanced forest growth. *Proceedings of the National Academy of Sciences*, *111*, 9527–9532. https://doi.org/10.1073/pnas.1402333111

Farquhar, G. D., Ehleringer, J. R., & Hubick, K. T. (1989). Carbon isotope discrimination and photosynthesis. *Annual Review of Plant Physiology and Plant Molecular Biology*, *40*, 503–537. https://doi.org/10.1146/annurev.pp.40.060189.002443

Farquhar, G., O'Leary, M., & Berry, J. (1982). On the relationship between carbon isotope discrimination and the intercellular carbon dioxide concentration in leaves. *Australian Journal of Plant Physiology*, *9*, 121–137. https://doi.org/10.1071/PP9820121

Farquhar, G. D., & Sharkey, T. D. (1982). Stomatal conductance and photosynthesis. *Annual Review of Plant Physiology*, *33*, 317–345. https://doi.org/10.1146/annurev.pp.33.060182.001533

Felix, J. D., Elliott, E. M., & Shaw, S. L. (2012). Nitrogen isotopic composition of coal-fired power plant NO_x: Influence of emission controls and implications for global emission inventories. *Environmental Science & Technology*, *46*, 3528–3535. https://doi.org/10.1021/es203355v

Fernández-Martínez, M., Vicca, S., Janssens, I. A., Ciais, P., Obersteiner, M., Bartrons, M., … Wang, X. (2017). Atmospheric deposition, CO_2, and change in the land carbon sink. *Scientific Reports*, *7*, 9632. https://doi.org/10.1038/s41598-017-08755-8

Francey, R. J., Allison, C. E., Etheridge, D. M., Trudinger, C. M., Enting, I. G., Leuenberger, M., … Steele, L. P. (1999). A 1000-year high precision record of $\delta^{13}C$ in atmospheric CO_2. *Tellus Series B*, *51*, 170–193. https://doi.org/10.3402/tellusb.v51i2.16269

Franks, P. J., Adams, M. A., Amthor, J. S., Barbour, M. M., Berry, J. A., Ellsworth, D. S., … Norby, R. J. (2013). Sensitivity of plants to changing atmospheric CO_2 concentration: From the geological past to the next century. *New Phytologist*, *197*, 1077–1094. https://doi.org/10.1111/nph.12104

Friedlingstein, P., Cox, P., Betts, R., Bopp, L., von Bloh, W., Brovkin, V., … Bala, G. (2006). Climate-carbon cycle feedback analysis: Results from the C4MIP model intercomparison. *Journal of Climate*, *19*, 3337–3353. https://doi.org/10.1175/JCLI3800.1

Gerhart, L. M., & McLauchlan, K. K. (2014). Reconstructing terrestrial nutrient cycling using stable nitrogen isotopes in wood. *Biogeochemistry*, *120*, 1–21. https://doi.org/10.1007/s10533-014-9988-8

Granda, E., Rossatto, D. R., Camarero, J. J., Voltas, J., & Valladares, F. (2014). Growth and carbon isotopes of Mediterranean trees reveal contrasting responses to increased carbon dioxide and drought. *Oecologia*, *174*, 307–317. https://doi.org/10.1007/s00442-013-2742-4

Greaver, T. L., Sullivan, T. J., Herrick, J. D., Barber, M. C., Baron, J. S., Cosby, B. J., … Herlihy, A. T. (2012). Ecological effects of nitrogen and sulfur air pollution in the US: What do we know? *Frontiers in Ecology and the Environment*, *10*, 365–372. https://doi.org/10.1890/110049

Gurmesa, G. A., Lu, X., Gundersen, P., Fang, Y., Mao, Q., Hao, C., & Mo, J. (2017). Nitrogen input ^{15}N signatures are reflected in plant ^{15}N natural abundances in subtropical forests in China. *Biogeosciences*, *14*, 2359–2370. https://doi.org/10.5194/bg-14-2359-2017

Hamburg, S. P., & Cogbill, C. V. (1988). Historical decline of red spruce populations and climatic warming. *Nature*, *331*, 428–431. https://doi.org/10.1038/331428a0

Hietz, P., Dünisch, O., & Wanek, W. (2010). Long-term trends in nitrogen isotope composition and nitrogen concentration in Brazilian rainforest trees suggest changes in nitrogen cycle. *Environmental Science & Technology*, *44*, 1191–1196. https://doi.org/10.1021/es901383g

Hobbie, E. A., & Högberg, P. (2012). Nitrogen isotopes link mycorrhizal fungi and plants to nitrogen dynamics. *New Phytologist*, *196*, 367–382. https://doi.org/10.1111/j.1469-8137.2012.04300.x

Homer, C., Dewitz, J., Yang, L., Jin, S., Danielson, P., Xian, G., … Megown, K. (2015). Completion of the 2011 national land cover database for the conterminous United States-representing a decade of land cover change information. *Photogrammetric Engineering and Remote Sensing*, *81*, 345–354.

Hyvönen, R., Ågren, G. I., Linder, S., Persson, T., Cotrufo, M. F., Ekblad, A., … Kellomäki, S. (2007). The likely impact of elevated $[CO_2]$, nitrogen deposition, increased temperature and management on carbon sequestration in temperate and boreal forest ecosystems: A literature review. *New Phytologist*, *173*, 463–480. https://doi.org/10.1111/j.1469-8137.2007.01967.x

Jennings, K. A., Guerrieri, R., Vadeboncoeur, M. A., & Asbjornsen, H. (2016). Response of *Quercus velutina* growth and water use efficiency to climate variability and nitrogen fertilization in a temperate deciduous forest in the northeastern USA. *Tree Physiology*, *36*, 428–443. https://doi.org/10.1093/treephys/tpw003

Johnson, S. E., & Abrams, M. D. (2009). Age class, longevity and growth rate relationships: Protracted growth increases in old trees in the eastern United States. *Tree Physiology*, *29*, 1317–1328. https://doi.org/10.1093/treephys/tpp068

Johnson, A. H., Cook, E. R., & Siccama, T. G. (1988). Climate and red spruce growth and decline in the northern Appalachians. *Proceedings of the National Academy of Sciences*, *85*, 5369–5373. https://doi.org/10.1073/pnas.85.15.5369

Johnson, A. H., & Siccama, T. G. (1983). Acid deposition and forest decline. *Environmental Science and Technology*, *17*, A294–A305. https://doi.org/10.1021/es00113a717

Joos, F., Prentice, I. C., & House, J. I. (2002). Growth enhancement due to global atmospheric change as predicted by terrestrial ecosystem models: Consistent with US forest inventory data. *Global Change Biology*, *8*, 299–303. https://doi.org/10.1046/j.1354-1013.2002.00505.x

Keeling, R. F., Piper, S. C., Bollenbacher, A. F., & Walker, S. J. (2010). Monthly atmospheric $^{13}C/^{12}C$ isotopic ratios for 11 SIO stations. In *Trends: A compendium of data on global change*. Oak Ridge, TN: Carbon Dioxide Information Analysis Center, Oak Ridge National Laboratory, U.S. Department of Energy.

Keeling, R. F., Piper, S. C., Bollenbacher, A. F., & Walker, S. J. (2015). *Scripps CO_2 Program*. Scripps Institution of Oceanography, University of California - San Diego, USA 92093-0244.

Keenan, T. F., Hollinger, D. Y., Bohrer, G., Dragoni, D., Munger, J. W., Schmid, H. P., & Richardson, A. D. (2013). Increase in forest water-use efficiency as atmospheric carbon dioxide concentrations rise. *Nature*, *499*, 324–327. https://doi.org/10.1038/nature12291

Kellndorfer, J., Walker, W., Kirsch, K., Fiske, G., Bishop, J., LaPoint, L., … Westfall, J. (2012). *NACP aboveground biomass and carbon baseline data (NBCD 2000)*.

Knauer, J., Zaehle, S., Reichstein, M., Medlyn, B. E., Forkel, M., Hagemann, S., & Werner, C. (2016). The response of ecosystem water-use efficiency to rising atmospheric CO_2 concentrations: Sensitivity and large-scale biogeochemical implications. *New Phytologist*, *213*, 1654–1666.

Kwak, J.-H., Lim, S.-S., Chang, S. X., Lee, K.-H., & Choi, W.-J. (2011). Potential use of $\delta^{13}C$, $\delta^{15}N$, N concentration, and Ca/Al of *Pinus densiflora* tree rings in estimating historical precipitation pH. *Journal of Soils and Sediments*, *11*, 709–721. https://doi.org/10.1007/s11368-011-0355-2

Kwak, J. H., Lim, S. S., Lee, K. S., Viet, H. D., Matsushima, M., Lee, K. H., … Choi, W. J. (2016). Temperature and air pollution affected tree ring $\delta^{13}C$ and water-use efficiency of pine and oak trees under rising CO_2 in a humid temperate forest. *Chemical Geology*, *420*, 127–138. https://doi.org/10.1016/j.chemgeo.2015.11.015

Lawrence, G. B., Hazlett, P. W., Fernandez, I. J., Ouimet, R., Bailey, S. W., Shortle, W. C., … Antidormi, M. R. (2015). Declining acidic deposition begins reversal of forest-soil acidification in the Northeastern U.S. and Eastern Canada. *Environmental Science and Technology*, *49*, 13103–13111. https://doi.org/10.1021/acs.est.5b02904

Le Quéré, C., Andrew, R. M., Friedlingstein, P., Sitch, S., Pongratz, J., Korsbakken, J. I., … , & Chini, D. Z. Z. (2018). The global carbon budget 2017. *Earth System Science Data*, *10*, 405–448.

Leavitt, S. W., & Long, A. (1982). Evidence for $^{13}C/^{12}C$ fractionation between tree leaves and wood. *Nature*, *298*, 742–744. https://doi.org/10.1038/298742a0

Lefohn, A. S., Husar, J. D., & Husar, R. B. (1999). Estimating historical anthropogenic global sulfur emission patterns for the period 1850–1990. *Atmospheric Environment*, *33*, 3435–3444. https://doi.org/10.1016/S1352-2310(99)00112-0

Leonelli, G., Battipaglia, G., Siegwolf, R. T. W., Saurer, M., Morra di Cella, U., Cherubini, P., & Pelfini, M. (2012). Climatic isotope signals in tree rings masked by air pollution: A case study conducted along the Mont Blanc Tunnel access road (Western Alps, Italy). *Atmospheric Environment*, *61*, 169–179. https://doi.org/10.1016/j.atmosenv.2012.07.023

Levesque, M., Andreu-Hayles, L., & Pederson, N. (2017). Water availability drives gas exchange and growth of trees in northeastern US, not elevated CO_2 and reduced acid deposition. *Scientific Reports*, *7*, 46158. https://doi.org/10.1038/srep46158

Lévesque, M., Siegwolf, R., Saurer, M., Eilmann, B., & Rigling, A. (2014). Increased water-use efficiency does not lead to enhanced tree growth under xeric and mesic conditions. *New Phytologist*, *203*, 94–109. https://doi.org/10.1111/nph.12772

Li, L., Yu, Z., Bebout, G. E., Stretton, T., Allen, A., & Passaris, P. (2010). Tree-ring width and $\delta^{13}C$ records of industrial stress and recovery in Pennsylvania and New Jersey forests: Implications for CO_2 uptake by temperate forests. *Chemical Geology*, *273*, 250–257. https://doi.org/10.1016/j.chemgeo.2010.02.026

Likens, G. E., Driscoll, C. T., & Buso, D. C. (1996). Long-term effects of acid rain: Response and recovery of a forest ecosystem. *Science*, *272*, 244–246. https://doi.org/10.1126/science.272.5259.244

Liu, S., Bond-Lamberty, B., Hicke, J. A., Vargas, R., Zhao, S., Chen, J., … Xiao, J. (2011). Simulating the impacts of disturbances on forest carbon cycling in North America: Processes, data, models, and challenges. *Journal of Geophysical Research*, *116*, G00K08.

Long, S. P., Ainsworth, E. A., Rogers, A., & Ort, D. R. (2004). Rising atmospheric carbon dioxide: Plants FACE the future*. *Annual Review of Plant Biology*, *55*, 591–628. https://doi.org/10.1146/annurev.arplant.55.031903.141610

Luo, Y., & Reynolds, J. F. (1999). Validity of extrapolating field CO_2 experiments to predict carbon sequestration in natural ecosystems. *Ecology*, *80*, 1568–1583. https://doi.org/10.1890/0012-9658(1999)080[1568:VOEFCE]2.0.CO;2

Luo, Y., Su, B. O., Currie, W. S., Dukes, J. S., Finzi, A., Hartwig, U., … Pataki, D. E. (2004). Progressive nitrogen limitation of ecosystem responses to rising atmospheric carbon dioxide. *BioScience*, *54*, 731. https://doi.org/10.1641/0006-3568(2004)054[0731:PNLOER]2.0.CO;2

McCarroll, D., & Loader, N. J. (2004). Stable isotopes in tree rings. *Quaternary Science Reviews*, *23*, 771–801. https://doi.org/10.1016/j.quascirev.2003.06.017

McDowell, N. G., Bond, B. J., Dickman, L. T., & Ryan, M. G. (2011). *Size- and age-related changes in tree structure and function*, Vol. *4*. Dordrecht, Netherlands: Springer Science & Business Media.

McLauchlan, K. K., Gerhart, L. M., Battles, J. J., Craine, J. M., Elmore, A. J., Higuera, P. E., … Perakis, S. S. (2017). Centennial-scale reductions in nitrogen availability in temperate forests of the United States. *Scientific Reports*, *7*, 7856. https://doi.org/10.1038/s41598-017-08170-z

McMahon, S. M., Parker, G. G., & Miller, D. R. (2010). Evidence for a recent increase in forest growth. *Proceedings of the National Academy of Sciences*, *107*, 3611–3615. https://doi.org/10.1073/pnas.0912376107

Muggeo, V. M. R. (2008). *Segmented: an R package to fit regression models with broken-line relationships*. 20–25.

Nadelhoffer, K., & Fry, B. (1994). Nitrogen isotope studies in forest ecosystems. In R. Michener & K. Lajtha (Eds.), *Stable isotopes in ecology and environmental science* (pp. 23–44). Hoboken, NJ: Wiley-Blackwell.

National Atmospheric Deposition Program (2015) *NTN data access*.

NOAA (2017). *National Centers for Environmental Information, West Virginia climate region 4 meteorological data*. 1895–2016.

Norby, R. J., DeLucia, E. H., Gielen, B., Calfapietra, C., Giardina, C. P., King, J. S., … De Angelis, P. (2005). Forest response to elevated CO_2 is conserved across a broad range of productivity. *Proceedings of the National Academy of Sciences*, *102*, 18052–18056. https://doi.org/10.1073/pnas.0509478102

Pan, Y., Birdsey, R. A., Fang, J., Houghton, R., Kauppi, P. E., Kurz, W. A., … Ciais, P. (2011). A large and persistent carbon sink in the world's forests. *Science*, *333*, 988–993. https://doi.org/10.1126/science.1201609

Pardo, L. H., Hemond, H. F., Montoya, J. P., Fahey, T. J., & Siccama, T. G. (2002). Response of the natural abundance of ^{15}N in forest soils and foliage to high nitrate loss following clear-cutting. *Canadian Journal of Forest Research*, *32*, 1126–1136. https://doi.org/10.1139/x02-041

Peñuelas, J., Canadell, J. G., & Ogaya, R. (2011). Increased water-use efficiency during the 20th century did not translate into enhanced tree growth. *Global Ecology and Biogeography*, *20*, 597–608. https://doi.org/10.1111/j.1466-8238.2010.00608.x

Piao, S., Friedlingstein, P., Ciais, P., Viovy, N., & Demarty, J. (2007). Growing season extension and its impact on terrestrial carbon cycle in the Northern Hemisphere over the past 2 decades. *Global Biogeochemical Cycles*, *21*, 1–11.

Pinheiro, J., Bates, D., DebRoy, S., Sarkar, D., & Team, R. C. (2018). *nlme: Linear and nonlinear mixed effects models*. R package version 3.1-131.1.

PRISM Climate Group (2004) *Oregon State University*. Retrieved from http://prism.oregonstate.edu

Richardson, A. D., Hollinger, D. Y., Dail, D. B., Lee, J. T., Munger, J. W., & O'Keefe, J. (2009). Influence of spring phenology on seasonal and annual carbon balance in two contrasting New England forests. *Tree Physiology*, *29*, 321–331. https://doi.org/10.1093/treephys/tpn040

Rinne, K. T. T., Loader, N. J. J., Switsur, V. R. R., Treydte, K. S. S., & Waterhouse, J. S. S. (2010). Investigating the influence of sulphur dioxide (SO_2) on the stable isotope ratios ($\delta^{13}C$ and $\delta^{18}O$) of tree rings. *Geochimica et Cosmochimica Acta*, *74*, 2327–2339. https://doi.org/10.1016/j.gca.2010.01.021

Santruckova, H., Santrucek, J., Setlik, J., Svoboda, M., & Kopacek, J. (2007). Carbon isotopes in tree rings of Norway spruce exposed to atmospheric pollution RID E-6860-2010. *Environmental science & technology*, *41*, 5778–5782. https://doi.org/10.1021/es070011t

Savard, M. M., Bégin, C., Parent, M., Smirnoff, A., & Marion, J. (2004). Effects of smelter sulfur dioxide emissions. *Journal of Environment Quality*, *33*, 13. https://doi.org/10.2134/jeq2004.1300

Schimel, D., Melillo, J., Tian, H., McGuire, A. D., Kicklighter, D., Kittel, T., … Parton, W. (2000). Contribution of increasing CO_2 and climate to carbon storage by ecosystems in the United States. *Science*, *287*, 2004–2006. https://doi.org/10.1126/science.287.5460.2004

Seibt, U., Rajabi, A., Griffiths, H., & Berry, J. A. (2008). Carbon isotopes and water use efficiency: Sense and sensitivity. *Oecologia*, *155*, 441–454. https://doi.org/10.1007/s00442-007-0932-7

Siccama, T. G., Bliss, M., & Vogelmann, H. W. (1982). Decline of red spruce in the green mountains of vermont. *Bulletin of the Torrey Botanical Club*, *109*, 162–168. https://doi.org/10.2307/2996256

Siccama, T. G., Hamburg, S. P., Arthur, M. A., Yanai, R. D., Bormann, F. H., & Likens, G. E. (1994). Corrections to allometric equations and plant tissue chemistry for hubbard brook experimental forest. *Ecology*, *75*, 246–248. https://doi.org/10.2307/1939398

Silva, L. C. R., Anand, M., & Leithead, M. D. (2010). Recent widespread tree growth decline despite increasing atmospheric CO_2 (ed Romanuk TN). *PLoS ONE*, *5*, e11543. https://doi.org/10.1371/journal.pone.0011543

Smith, K. R., Mathias, J. M., McNeil, B. E., Peterjohn, W. T., & Thomas, R. B. (2016). Site-level importance of broadleaf deciduous trees outweighs the legacy of high nitrogen (N) deposition on ecosystem N status of Central Appalachian red spruce forests. *Plant and Soil*, *408*, 343–356. https://doi.org/10.1007/s11104-016-2940-z

Sokal, R. R., & Rohlf, F. J. (2011). *Biometry*, 4th ed.. W. H: Freeman.

Spiess, A.-N. (2017) *Propagate: Propagation of uncertainty*. R package version 1.0-5.

Stokes, M. A., & Smiley, T. L. (1996). *An Introduction to Tree-Ring Dating*. Tuscon, AZ: University of Arizona Press.

Thomas, R. Q., Canham, C. D., Weathers, K. C., & Goodale, C. L. (2010). Increased tree carbon storage in response to nitrogen deposition in the US. *Nature Geoscience*, *3*, 13–17. https://doi.org/10.1038/ngeo721

Thomas, R. B., Spal, S. E., Smith, K. R., & Nippert, J. B. (2013). Evidence of recovery of *Juniperus virginiana* trees from sulfur pollution after the Clean Air Act. *Proceedings of the National Academy of Sciences*, *110*, 15319–15324. https://doi.org/10.1073/pnas.1308115110

USDA Soil Survey Geographic (SSURGO) (2015). *Database for Pocahontas and Randolph Counties, WV*. Washington, DC: USDA-Natureal Resources Conservation Service.

U.S. Environmental Protection Agency (2015). *Air emissions inventory, Air pollution emissions trends data*.

US Geological Survey (1946). *Physiographic divisions of the conterminous U.S.*

West Virginia Geological Economic Survey (1968). *Surface geology - Rock units*. Online Digitized Map. In: T.U. West Virginia DEP (Ed.), William and Heintz Corporation.

Whittaker, R. H., Bormann, F. H., Likens, G. E., & Siccama, T. G. (1974). The hubbard brook ecosystem study: Forest biomass and production. *Ecological Monographs*, *44*, 233–254. https://doi.org/10.2307/1942313

Wigley, T. M. L., Briffa, K. R., & Jones, P. D. (1984). On the average value of correlated time series, with applications in dendroclimatology and hydrometeorology. *Journal of Climate and Applied Meteorology*, *23*, 201–213. https://doi.org/10.1175/1520-0450(1984)023<0201:OTAVOC>2.0.CO;2

Zang, C., & Biondi, F. (2015). Treeclim: An R package for the numerical calibration of proxy-climate relationships. *Ecography*, *38*, 431–436. https://doi.org/10.1111/ecog.01335

Zeng, X., Liu, X., Xu, G., Wang, W., & An, W. (2014). Tree-ring growth recovers, but $\delta^{13}C$ and $\delta^{15}N$ do not change, after the removal of point-source air pollution: A case study for poplar (*Populus cathayana*) in northwestern China. *Environmental Earth Sciences*, *72*, 2173–2182. https://doi.org/10.1007/s12665-014-3127-7

SUPPORTING INFORMATION

Additional supporting information may be found online in the Supporting Information section at the end of the article.

How to cite this article: Mathias JM, Thomas RB. Disentangling the effects of acidic air pollution, atmospheric CO_2, and climate change on recent growth of red spruce trees in the Central Appalachian Mountains. *Glob Change Biol*. 2018;24:3938–3953. https://doi.org/10.1111/gcb.14273